Journal of Applied Polymer Science

Effects of Freezing Conditions on the Morphology and Mechanical Properties of Clay and Polymer/Clay Aerogels

Yuxin Wang, Matthew D. Gawryla, David A. Schiraldi
Department of Macromolecular Science & Engineering, Case Western Reserve University, Cleveland, Ohio 44106
Correspondence to: D. A. Schiraldi (E-mail: das44@case.edu)

ABSTRACT: Clay aerogels and poly(vinyl alcohol)/clay aerogels were prepared via an environmental friendly freeze-drying process. Both mechanical properties and microstructures of the clay aerogels and polymer/clay aerogels were correlated to the freezing conditions. The compressive moduli of these materials increased as the freezing temperature used to produce the aerogels was decreased. Scanning electron microscopic observations suggest that the morphological variations of clay aerogels can be explained by the mechanism of ice templating that produced these structures. © 2013 Wiley Periodicals, Inc. J. Appl. Polym. Sci. 129: 1637–1641, 2013

KEYWORDS: clay; composites; foams; structure–property relations; synthesis and processing

Received 1 January 2013; accepted 2 January 2013; published online 8 March 2013
DOI: 10.1002/app.39143

INTRODUCTION

Freeze-drying (lyophilization) has been widely used in the food and pharmaceutical industries because of its safety and minimal effect on both product and the environment. In this two step drying process, a solvent or solvent-wetted solid is frozen then subjected to high vacuum and progressively increasing heat, bringing about sublimation at an optimized rate.[1,2] Both heat transfer and mass transfer occur simultaneously, therefore in the freeze-drying process.[3] *Call* first reported the freeze-drying of clay-gels to produce what can be termed a clay aerogel.[4] Clay aerogels are ultra low density/high specific area materials due to their high porosity.[5] The use of this freeze-drying method can be extended into the polymer field to prepare foam-like polymer aerogels; incorporation of clays and other fillers into the polymer aerogel systems can substantially improve their mechanical properties by imposing highly regular, "house of cards" or fractal structures.[6] A series of recent publications have demonstrated that water-based polymer/clay aerogels can be developed for potential applications including thermal insulation, packaging, and animal waste absorption; the most desirable solvent to be used in such a freeze-drying process is water, from an environmental point of view.[7–9] The freezing process for the preparation aerogels in this manner can be regarded as proceeding via ice crystallization; as the ice crystals nucleate and grow, the inorganic filler, and polymer molecules are pushed to the interstitial regions in between those ice crystals.[10–12] The drying process leaves a residual structure of the ice crystal grain boundaries as the solid matter in the finished material.

Aerogel structures can be changed by varying polymer: clay ratios and individual concentrations as well as polymer and clay types.[13] Freezing is the determinant step for the morphology of a group of aerogels with fixed compositions. X-ray studies have been carried out on sodium montmorillonite samples before and after freeze-drying into an aerogel, showing that the main reduction in interlayer spacing of the clay takes place upon freezing.[14] Nakazawa et al. has reported a correlation between freezing rates and aerogel morphology, with pore shapes changing from polygonal cells to thin lenses.[15] Ohta and Nakazawa tested the compressive strength of porous clay/organic composites, concluding that compressive strengths increase with decreasing pore diameters.[16] O'Brien et al. proposed that freezing steps in the preparation of collagen-GAG scaffolds carried out at a constant freezing rate could provide a more homogenous pore size than when a rapid super quench freezing process was used, which would instead lead to scaffold heterogeneity.[17] Svagan et al., whose study focused on starch-based biofoams, suggested a relationship between mechanical properties and cell structure and cell wall compositions. A lower aerogel preparation temperature would be expected to result in scaffolds with smaller and more numerous cells, based on the current literature, in turn translating to higher Young's moduli, yield strengths, and toughness in these materials.[18]

The current work examines the relationship between freezing conditions and compressive mechanical properties in clay and polymer/clay aerogels, providing a fundamental understanding about aerogel formation, and contributing to the body of practical knowledge needed for commercial exploitation of this field.

Applied Polymer SCIENCE

Table I. Preparation of Cooling Baths[19]

Condition no.	Temperature (°C)	Compositions
1	−23	CCl_4/CO_2 (s)
2	−41	Acetonitrile/CO_2 (s)
3	−56	*n*-Octane/CO_2 (s)
4	−77	Ethanol/CO_2 (s)
5	−95	Acetone/N_2(l)
6	−116	Ethanol/N_2(l)
7	−131	*n*-Pentane/N_2(l)
8	−172	CO_2 (s)/N_2(l)

EXPERIMENTAL

Materials

Sodium montmorillonite clay (Nanocor PGW grade, Na-MMT), poly(vinyl alcohol) (PVOH, Sigma Aldrich) with a molecular weight range of 31,000–50,000 and the freezing bath solvents listed in Table I were used as received or prepared. Deionized water (DI water) was prepared using a Barnstead RoPure reverse osmosis system.

Aerogel Formation

Five grams of Na-MMT was mixed with 100 mL DI water in a Waring laboratory blender to prepare 5% wt/vol clay suspension. This suspension was then transferred to 18 mL polystyrene cylindrical vials with a diameter of 20 mm and frozen using the different cooling baths shown in Table I. PVOH was dissolved in DI water at 90°C to prepare a 10% wt/vol solution, as previously described.[20] Na-MMT was mixed with DI water in the blender to produce a 10% wt/vol suspension. Equal volumes of PVOH solution and clay suspension were mixed using a low shear rate hand mixer for 30 min, followed by stirring with a magnetic stir bar at 70°C for 2 h then overnight at room temperature to form a 5% wt/vol PVOH 5% wt/vol clay suspension. Polymer/clay suspensions were then frozen by immersing the vials into the cooling baths described above for anisotropic freezing. The samples were then freeze-dried using a Virtis Advantage EL-85 lyophilizer with an initial shelf temperature of 25°C, condenser temperature of −80°C and an ultimate 5 μm bar vacuum.

Morphology

The microstructures of clay aerogels were imaged using an FEI Quanta 3D scanning electron microscope. Prior to imaging, all samples were sputter coated with gold and were studied with the microscope operating at 5 kV. Also, one clay aerogel sample frozen in an ethanol/solid CO_2 bath was embedded in epoxy; during this process the aerogel was placed under vacuum while epoxy was added drop by drop to penetrate the whole sample without damaging it prior to microtoming and further investigation using a JEOL JEM-1200 EX transmission electron microscope (TEM). For this measurement, the TEM instrument was operated at an accelerating voltage of 5 kV.

Mechanical Testing

The aerogels were cut by bandsaw to create 20 mm diameter by 20 mm height samples. Compressive tests were carried out using an Instron 5566 Universal testing machine with a crosshead speed of 1 mm/min.

RESULTS AND DISCUSSIONS

Morphology of Clay and PVOH/Clay Aerogels

The freezing process is a dynamic, kinetic process, relying on both the external freezing temperature, and the internal viscosity. In our research, the freezing temperature is the only variable. Clay and PVOH/clay aerogels were successfully produced according to the method described herein. Regardless of freezing conditions employed, freeze-drying of 5 wt % clay gels resulted in aerogels with bulk densities of 0.05 g/cm^3; freeze-drying of 5 wt % clay/5 wt % PVOH gels similarly produced aerogels with bulk densities of 0.10 g/cm^3.

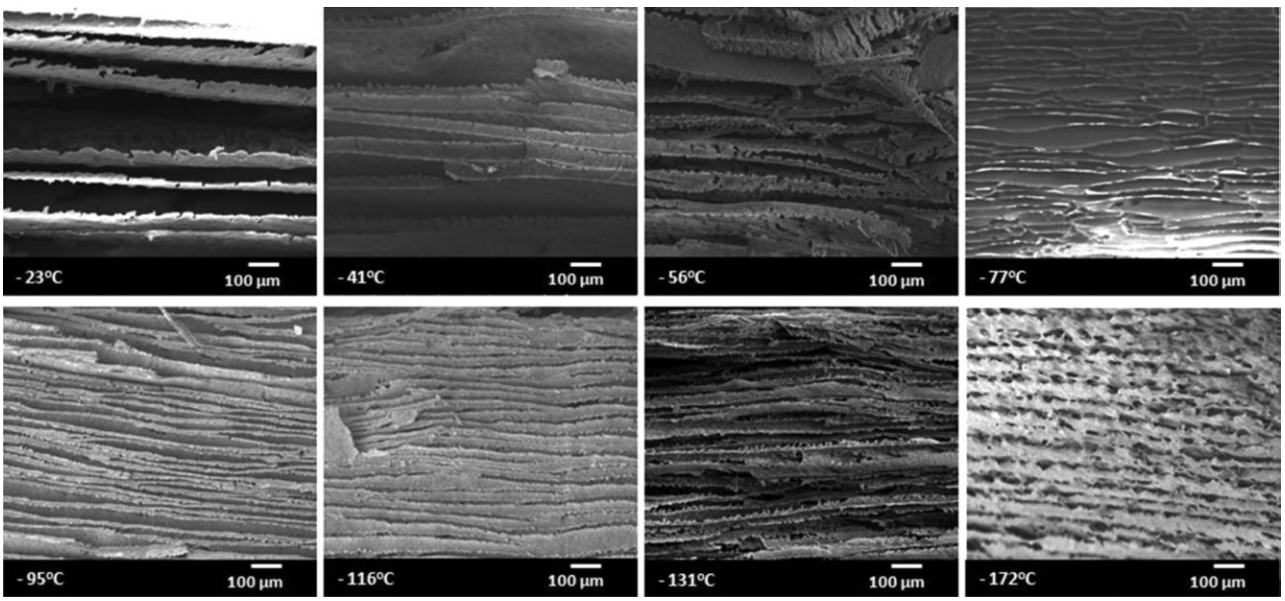

Figure 1. SEM images of clay aerogel frozen at different freezing temperatures.

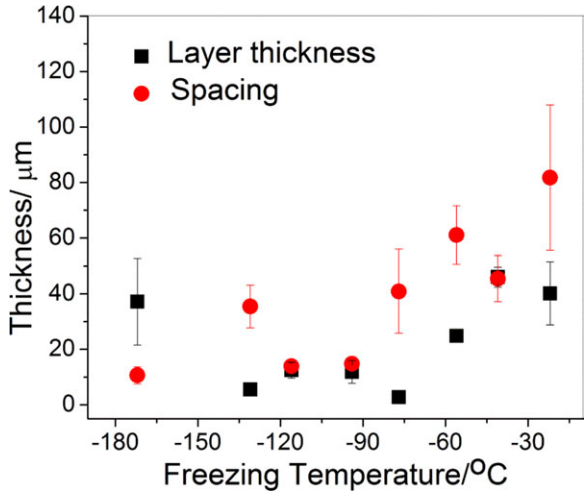

Figure 2. Clay aerogel layer thickness and spacing at different freezing temperatures. [Color figure can be viewed in the online issue, which is available at wileyonlinelibrary.com.]

The clay aerogels exhibited layered structures as shown in Figure 1; each set of conditions produced layered, ice-templated structures, which of clay aerogel can be correlated to thin lens structure described by Nakazawa et al.[15] Both the layer thicknesses and interlayer spacing varied as the freezing temperature was changed. Since, clay aerogels display the negative of the ice crystal structures (i.e., their grain boundaries), both layer thickness and interlayer spacing can be attributed to ice crystallization with its nucleation and growth. Ice nucleation will generally begin near the coldest surface, and the colder that surface is, the more heterogeneous nuclei will form at the beginning.[11,12] This phenomenon can explain the decreasing trend in both layer thickness and spacing that was observed in the present study. Growing ice fronts move in a direction opposite to that of heat transfer so as to guide the formation of clay regions.[21] The growing ice will push the clay aside and into its grain boundaries. When ice growth wins over ice nucleation as the more significant process and becomes the predominate step, under steady state conditions, ice fronts will move at a constant rate, producing high aspect ratio, homogenous layered clay aerogels. Since, the ice freezing direction is uncontrollable in our experiment, it is expected that the ice crystals were formed randomly. Various freezing temperatures would contribute to different ice crystal sizes. Low temperature/high pressure conditions and high freezing rate reduces the time for ice crystal growth so as to produce smaller crystals.[22]

As the freezing temperature was reduced from −23 to −77°C, the layer thicknesses decreased from an average of 45 to 3 μm (Figure 2). Further reducing the freezing temperature to −172°C resulted in an increase of layer thickness from 12 to 37 μm. The interlayer spacing exhibited a similar trend of decreasing with lower freezing temperature.

When aqueous PVOH/clay mixtures were frozen at different temperatures, the resultant aerogels exhibited both layered structure (similar to those produced in clay-only aerogels) and evenly-dispersed small pores in each layer (Figure 3). Different from clay gels, the viscosity change in the initial PVOH/clay mixtures weakened the dominant effect from ice propagation and led to the competition between ice nucleation and propagation steps. Therefore, the polymer-clay-water interaction during ice crystallization hinders some ice growth into large platelets rather than small ice crystalline. The layer thicknesses in these structures show a decreasing trend as temperature decreases from −23 to −172°C (Figure 4). It is evident that the layer thickness could be controlled in the range of a few micrometers to 100 μm. It is difficult to accurately measure interlayer spacing in these polymer/clay aerogels, as a great deal of inter-connectivity is present.

Samples imaged by scanning electron microscope (SEM) were torn from the original aerogel samples while for TEM imaging;

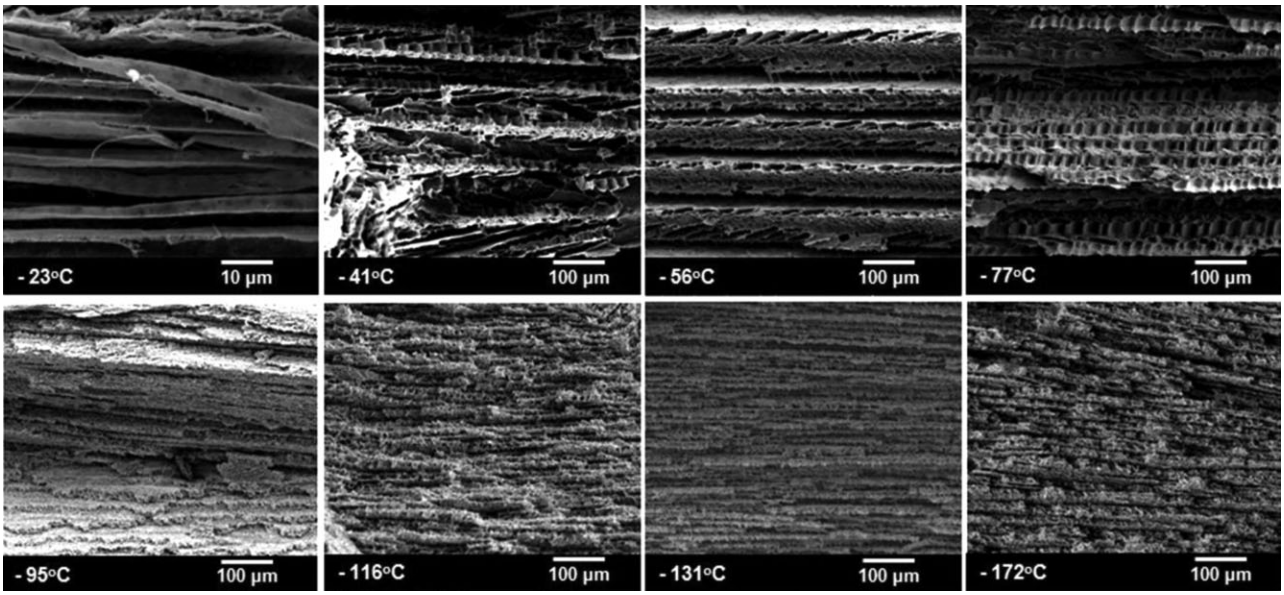

Figure 3. SEM images of PVOH/clay aerogel frozen at different freezing temperatures.

Applied Polymer SCIENCE

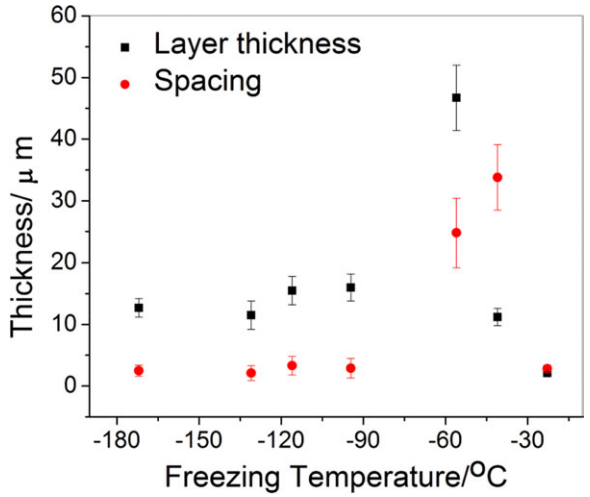

Figure 4. PVOH/Clay aerogel layer thickness and spacing at different freezing temperatures. [Color figure can be viewed in the online issue, which is available at wileyonlinelibrary.com.]

these fragile samples were protected by epoxy and microtomed, resulting in less damage. Figures 5(a,b) shows TEM images of clay aerogel prepared at −77°C. The single layer thickness is estimated to be 100–200 nm while the interlayer spacing is 10–15 μm. The measurement from SEM images Figure 5(c) indicates that the layer thickness is (2.8 ± 1.0) μm while the spacing is (41 ± 15) μm. The differences in SEM and TEM likely result from both sample preparation and equipment limitations. The layer thicknesses measured by SEM are much larger than that of the exfoliated single clay platelets considering the hierarchical structure of clay aerogel; the resolution differences provided by TEM allow for analysis of packing patterns between each clay platelets, which appear to be packed next to each other in a "ric-rac" pattern causes the undulating clay layer structures observed in both SEM and TEM images. The relatively larger measured values from SEM might be also due to this inaccuracy which results from the aforementioned undulations.

Compressive Properties of Clay and PVOH/Clay Aerogels

With decreasing freezing temperatures, both the clay aerogels and the PVOH/clay aerogel exhibited increasing trends in their compressive moduli. Narrower interlayer spacing and thinner layer thicknesses translated to more compacted structures, which should yield more rigid composites. The compressive modulus of a PVOH/clay aerogel is two orders of magnitude higher than that of a comparably-produced clay aerogel (Figures 6 and 7). The polymer/clay aerogel moduli are comparable to those of expanded polystyrene foams, for which we measure a compressive modulus of 3 MPa for a typical commercial grade used for packaging electronic goods. By decreasing the freezing temperature used for producing a PVOH/clay aerogel, we can adjust the product modulus within the range of 4–7 MPa by optimizing the packing geometries of clay platelets in the composite. It should be noted that variability in aerogel samples, and therefore in compressive mechanical properties are greater than are typical in extruded or injection molded samples, and typically are in the range of ±10% in our experience, making multiple sample testing extremely important.

The compressive moduli of both clay aerogels and PVOH/clay aerogels prepared at −116°C deviated from the general trend and exhibited less variability as well. The standard deviation in mechanical properties of aerogels is attributed to the aerogel morphology especially the pore size, which is derived from the various ice crystal forms.[23] Water exhibits a T_g of −137°C and an unusual fragile-to-strong transition in viscosity within this region.[24,25] Therefore, when the water mixtures are frozen near this temperature, the temperature-induced viscosity change in water could restrict the ice crystal propagation so as to impact the mobility of polymer chain and nanoparticle, which contributes to the molecular-morphology change, therefore influence the mechanical properties. Though these changes are unable to be detected by SEM, it may be indirectly confirmed by small angle neutron scattering via characterization of their fractal volume.[26] Other than mechanical properties, this phenomenon may also contribute to other important properties change in clay aerogel, such as their skeletal density and thermo-conductivity, which may be of great interest for future study. It should be noted that the variability of the compressive moduli results are more variable than ideal, reflecting the reality of aerogel structural variability—these result are nonetheless directionally useful and provide guidance to both fundamental understanding and practical production of optimized aerogels.

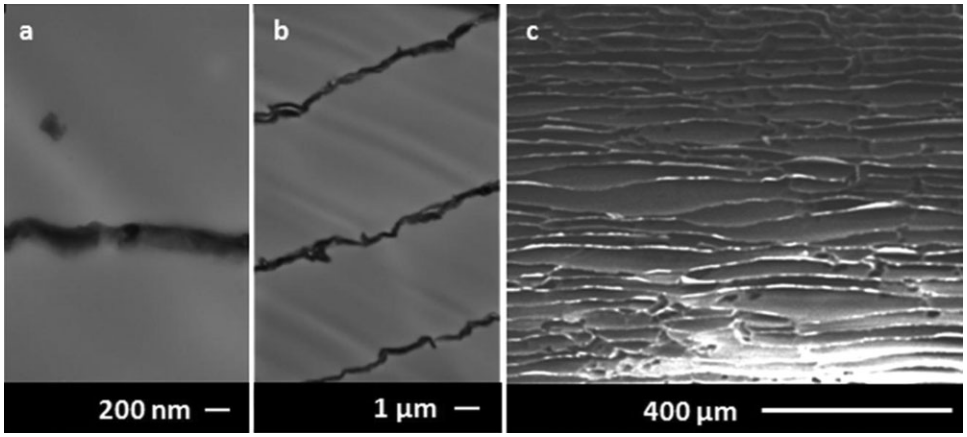

Figure 5. Microstructures of clay aerogel frozen at (a and b) −77°C via TEM and (c) SEM.

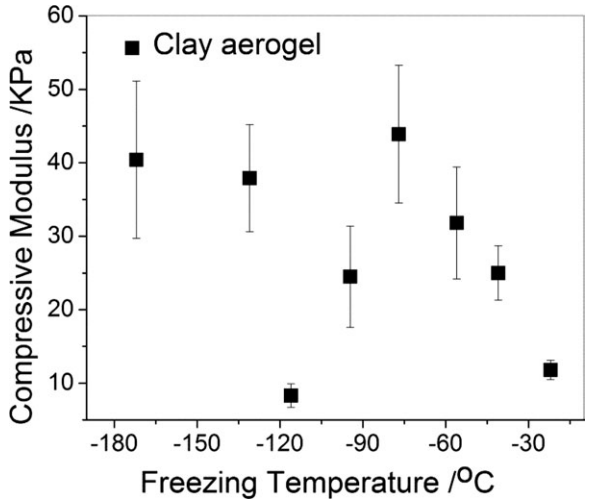

Figure 6. Compressive modulus of clay aerogel produced at different freezing temperatures.

CONCLUSIONS

Clay aerogels were fabricated via a freeze-drying process. Poly (vinyl alcohol)/clay aerogels were also prepared as a typical example of water-soluble polymer/clay aerogels. The freezing process plays a key role in controlling the morphology and compressive properties of these samples; as the freezing temperature decreased, the compressive modulus showed a general increasing trend with more compacted aerogel layers and a decreasing layer thickness. The observed structure/property versus temperature trends can be explained by the formation of a greater number of ice nuclei when lower freezing temperatures are used in the process.

ACKNOWLEDGMENTS

Financial support from the Case School of Engineering is acknowledged. Assistance on TEM imaging by Midori Hitomi is greatly appreciated. One of the coauthors, Dr. David Schiraldi, has a financial interest in a company that is commercializing the technology investigated in this research. He is an owner and officer of the company. Case Western Reserve University also has an ownership and IP interest in this technology which, if commercialized, could result in royalties for Dr. Schiraldi and CWRU.

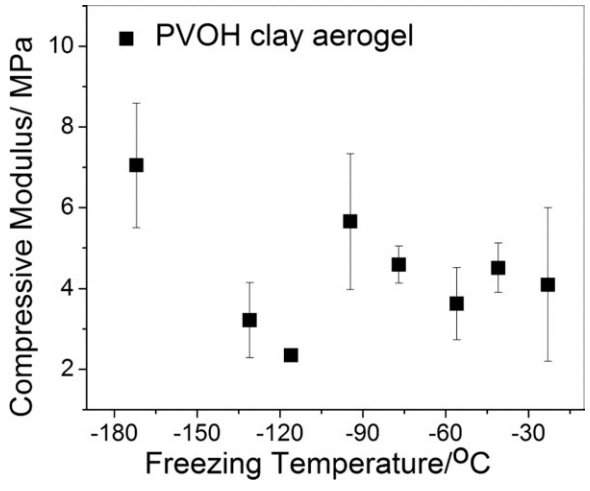

Figure 7. Compressive modulus of PVOH clay aerogel produced at different freezing temperatures.

REFERENCES

1. Liu, Y.; Zhao, Y.; Feng, X. *Appl. Therm. Eng.* **2008**, *28*, 675.
2. Searles, J. A.; Carpenter, J. F.; Randolph, T. W. *J. Pharm. Sci.* **2001**, *90*, 860.
3. Kochs, M.; Korber, C. H.; Nunner, B.; Heschel, I. *Heat Mass Transfer* **1991**, *34*, 2395.
4. Call, F. *Nature* **1953**, *172*, 126.
5. Schubert, U.; Husing, N. *Angew. Chem. Int. Ed.* **1998**, *37*, 22.
6. Bandi, S.; Bell, M.; Schiraldi, D. A. *Macromolecules* **2005**, *38*, 9216.
7. Gawryla, M. D.; Nezamzadeh, M.; Schiraldi, D. A. *Green Chem.* **2008**, *10*, 1078.
8. Gawryla, M. D.; Schiraldi, D. A. *Macromol. Mater. Eng.* **2009**, *294*, 570.
9. Hostler, S. R.; Abramson, A. R.; Gawryla, M. D.; Bandi, S.; Schiraldi, D. A. *Int. J. Heat Mass Transfer* **2009**, *52*, 665.
10. Jennings, T. A. Lyophilization: Introduction and Basic Principles; Interpharm CRC: Boca Raton, **1999**.
11. Gutierrez, M. C.; Ferrer, M. L.; del Monte, F. *Chem. Mater.* **2008**, *20*, 634.
12. Deville, S.; Saiz, E.; Nalla, R. K.; Tomsia, A. P. *Science* **2006**, *311*, 515.
13. Colard, C. A. L.; Cave, R. A.; Grossiord, N.; Covington, J. A.; Bon, S. A. F. *Adv. Mater.* **2009**, *21*, 2894.
14. Norrish, K.; Rausell-Colom, J. A. *Clay Miner. Bull.* **1963**, *5*, 9.
15. Nakazawa, H.; Yamada, T.; Fujita, T.; Ito, Y. *Clay Sci.* **1987**, *6*, 269.
16. Ohta, S.; Nakazawa, H. *Appl. Clay Sci.* **1995**, *9*, 425.
17. O'Brien, F. J.; Harley, B. A.; Yannas, I. V.; Gibson, L. J. *Biomaterials* **2004**, *25*, 1077.
18. Svagan, A. J.; Jensen, P.; Berglund, L. A.; Dvinskikh, S. V.; Furo, I. J. *J. Mater. Chem.* **2010**, *20*, 4321.
19. Cooling Baths. http://www2.bc.edu/∼ hoveyda/cool.html (accessed 07/05/2012).
20. Alhassan, S. M.; Qutubuddin, S.; Schiraldi, D. A. *Langmuir* **2010**, *26*, 12198.
21. Zhang, H.; Hussain, I.; Brust, M.; Butler, M. F.; Rannard, S. P.; Cooper A. I. *Nat. Mater.* **2005**, *4*, 787.
22. Ren, L.; Tsuru, K.; Hayakawa, S.; Osaka, A. *Biomaterials* **2002**, *23*, 4765.
23. Water Structure and Science. http://www.lsbu.ac.uk/water/index2.html (accessed 07/05/2012).
24. Velikov, V.; Borick, S.; Angell, C. A. *Science* **2001**, *14*, 2335.
25. Tanaka, H. *J. Phys.: Condens. Matter*, **2003**, *15*, 703.
26. Reidy, R. F.; Allen, A. J.; Krueger, S. *J. Non Cryst. Solids* **2001**, *285*, 181.